Refined acoustic modeling and analysis of shotgun microphones

Mingsian R. Bai[a] and Yi-Yang Lo
Department of Power Mechanical Engineering, National Tsing Hua University, No. 101, Section 2, Kuang-Fu Road, Hsinchu 30013, Taiwan

(Received 1 July 2012; revised 22 January 2013; accepted 25 January 2013)

A shotgun microphone is a highly directional pickup device widely used in noisy environments. The key element that leads to its superior directivity is a tube with multiple slot openings along its length. One traditional way to model the directional response of a shotgun is to assume plane waves traveling in the tube as if it is in the free field. However, the frequency response and directivity predicted by this traveling wave model can differ drastically from practical measurements. In this paper, an in-depth electroacoustic analysis was conducted to examine the problem by considering the standing waves inside the tube with an analogous circuit containing phased pressure sources and T-networks of tube segments. A further refinement is to model the housing diffraction effect with the aid of the equivalent source method (ESM). The on-axis frequency response and directivity pattern predicted by the proposed model are in close agreement with the measurements. From the results, a peculiar bifurcation phenomenon of directivity pattern at the Helmholtz frequency was also noted. While the shotgun behaves like an endfire array above the Helmholtz frequency, it becomes a broadside array below the Helmholtz frequency. The standing wave effect can be mitigated by covering the slot openings with mesh screen, which was found to alter the shotgun response to be closer to that of the traveling wave model above a critical frequency predicted by the half-wavelength rule. A mode-switching model was developed to predict the directional responses of mesh-treated shotguns.
 [http://dx.doi.org/10.1121/1.4792147]

PACS number(s): 43.38.Hz, 43.38.Kb, 43.25.Gf [DDE] Pages: 2036–2045

I. INTRODUCTION

In this paper, the frequency and directional responses of shotgun microphones are studied by the standing-wave and interference phenomena. For many audio applications, it is necessary to use microphones with high-directionality.[1] In the film industry, for example, dialog pickup on the shooting set is usually done by way of high-directionality microphones. Sport events with high ambient noise level may require high-directionality microphones. Field recording of bird calls may call for operation at great distances with highly directional microphones. Shotgun microphones or line microphones are commonplace to achieve such high directionality.

The generic structure of a shotgun microphone consists of a microphone loaded with a tube with slot opening along its length. A shotgun microphone is highly directional in that it can focus on the target source and reject off-axis noise and interference. This directionality results from ingenious design of acoustic interference of the exterior filed at the openings and interior field in the tube. In the early development of shotgun microphones, the traveling-wave model (TWM) was suggested by Olson and Mason.[2–5] Olson analytically models directional microphones by integrating the delays of exterior field arriving at each orifice and propagating delays in the shotgun tube. Mason's approach to calculate delays is similar to the Olson's method except the use of discrete summation instead of continuous integration used by Olson. In their model, the exterior field is modeled as incoming plane waves and the interior field is modeled as traveling plane waves. To be specific, the exterior field model follows the phased array concept, which assumes that the plane waves are produced by a farfield source arrived at each slot opening with different times. For the internal field, the model assumed that sound waves entering the slot openings propagate and combine in the form of traveling plane waves to result in highly directionality of the shotgun microphone.

Following Olson and Mason's work, another shotgun microphone model was proposed by Carnes whose model is based on transfer matrices of the shotgun tube.[6] These developments of shotgun microphone were summarized in literature.[1,7] Dix extended the shotgun model based on Olson, Mason, and Carne's work. He modeled the shotgun loudspeakers by using the T-networks.[8]

Despite the widespread use of shotgun microphones, there remains much to explore in terms of theoretical aspects. In particular, the frequency response and directivity predicted by the preceding TWM can differ drastically from practical measurements in some cases. In this paper, an in-depth electroacoustic analysis is carried out to examine the problem by considering the standing waves inside the tube. This approach termed the standing-wave model (SWM) is based on an analogous circuit[8–11] containing phased pressure sources and T-network of tube sections. With the SWM, we are able to model the directional and on-axis frequency responses of shotgun microphones more accurately than the TWM. One interesting phenomenon derived from the SWM is the bifurcation of beam pattern at the Helmholtz frequency.

A further refinement is incorporated into the analysis by modeling the diffraction effect due to the housing. The equivalent source method (ESM)[12] is employed to calculate the diffraction pattern through the formulation of a reciprocal

[a]Author to whom correspondence should be addressed. Electronic mail: msbai@pme.nthu.edu.tw

problem. The combined SWM-ESM will predict the on-axis frequency response and directional response of the shotgun microphone with improved accuracy. A peculiar bifurcation phenomenon of directivity pattern observed in the results at the Helmholtz frequency will be investigated. In addition, it is seen from the measurement that mesh treatment to the slot openings has a significant impact on the shotgun responses. The standing wave effect can be mitigated by the mesh treatment; this not only increases the directivity index (DI) but also makes the shotgun response closer to that of the traveling wave model above a critical frequency predicted by the half-wavelength rule. For this scenario, a mode-switching model is developed in this work to better predict the responses of mesh-treated shotguns.

II. MODELING SHOTGUN MICROPHONES

In this section, theoretical background of shotgun microphones is given. First, the lumped-parameter model of a condenser microphone is reviewed. Next, the TWM of the shotgun tube is reviewed, followed by the SWM that gives more accurate prediction of the frequency and directional responses of shotgun microphones.

A. Microphone model

Prior to the discussion of the complete shotgun system, a brief review of the electroacoustic analogous circuit[9–11] of a condenser microphone is given in this section (Fig. 1). In the acoustical domain, the p_i denotes incident sound pressure and $S_D u_D$ is the volume velocity produced by the diaphragm with area S_D and average velocity u_D. The radiation impedance is given by

$$Z_{AR} = \left(\frac{1}{R_A} + \frac{1}{j\omega M_A}\right)^{-1}, \tag{1}$$

with

$$M_A = \frac{8\rho_0}{3\pi^2 r_D} \tag{2}$$

being the radiation mass and

$$R_A = \frac{128\rho_0 c}{9\pi^3 r_D^2} \tag{3}$$

being the radiation resistance, where r_D is the diaphragm radius, ρ_0 is the air density, and c is the speed of sound. Next the acoustical impedance of the air gap between the diaphragm and the backplate can be expressed as[18–20]

$$Z_a = \frac{12\eta}{N_b \pi h_a^3}\left(\frac{\gamma}{2} - \frac{\gamma^2}{8} - \frac{\ln(\gamma)}{4} - \frac{3}{8}\right), \tag{4}$$

where h_a is the air gap distance, η is the viscosity of air, N_b is the number of holes on the backplate, and γ is the surface fraction of the backplate occupied by the acoustical holes. The acoustical impedance of the backplate perforation[13] is

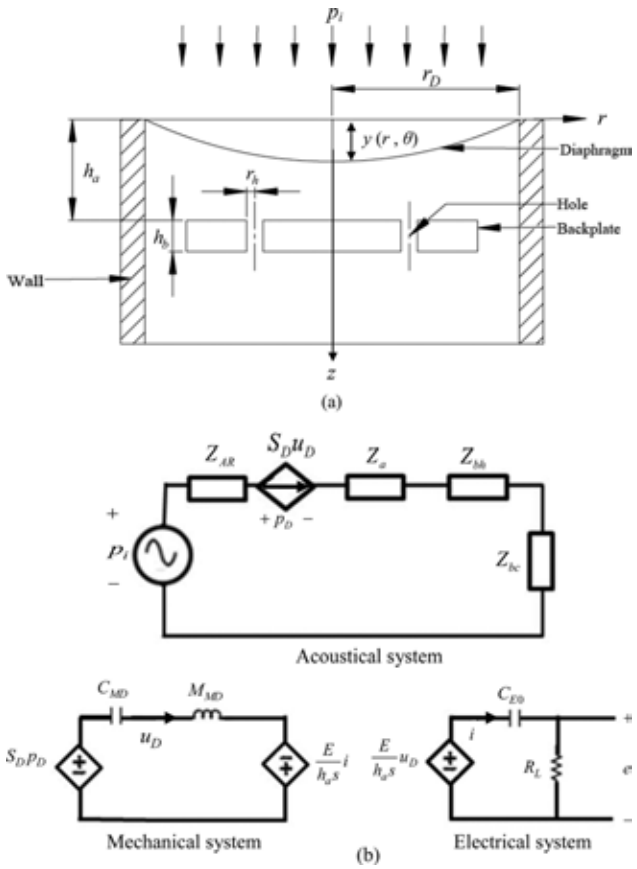

FIG. 1. Condenser microphone and the associated analogous circuits. (a) The cross section of a condenser microphone. (b) Electroacoustic analogous circuits.

$$Z_{bh} = \frac{8\eta h_b}{N_b \pi r_h^4}, \tag{5}$$

where r_h is the radius of the hole and h_b is the thickness of the backplate. The acoustical impedance of the back chamber[14,15] is given by

$$Z_{bc} = \frac{1}{j\omega C_{bc}}, \tag{6}$$

$$C_{bc} = \frac{V}{\rho_0 c^2}, \tag{7}$$

where C_{bc} is the acoustical compliance of the backchamber with volume V. The mechanical system is approximated by equivalent compliance and mass elements of the diaphragm as follows:[21]

$$C_{MD} = \frac{1}{8\pi T}, \tag{8}$$

$$M_{MD} = \frac{4\rho_d h_d}{3}, \tag{9}$$

where T is the tensile force per unit length, h_d is the diaphragm thickness, and ρ_d is the diaphragm density. In the electrical domain, C_{E0} is the quiescent capacitance between the diaphragm and the backplate. Assume that

$$R_L \gg \frac{1}{j\omega C_{E0}}. \tag{10}$$

From Ref. 10, the open-circuit sensitivity of the microphone can be shown to be

$$\frac{e_{om}(\omega)}{p_i} = \frac{E}{h_a}\frac{S_D}{j\omega(S_D^2 Z_A + Z_M)}, \tag{11}$$

$$Z_A = Z_a + Z_{bh} + Z_{bc}, \tag{12}$$

$$Z_M = j\omega M_{MD} + \frac{1}{j\omega C_{MD}}, \tag{13}$$

where $e_{om}(\omega)$ is the open circuit voltage and E is the polarization voltage.

B. Traveling-wave model

Traditionally, the TWM is commonly used to predict directional response of the shotgun microphone. In this section, we try to reformulate this model from the perspective of array signal processing. Assume that plane waves are emitted by a farfield source impinge on a tube with N_h slot opening along its length. The field exterior and interior to the tube are considered separately.

For the exterior field, the shotgun tube can be regarded as an N_h-element endfire array, as shown in Fig. 2. The plane waves propagating from the farfield to each hole correspond to the array manifold vector[22]

$$\mathbf{a} = [\,1 \quad e^{jkd_s\cos\theta} \quad \cdots \quad e^{jk(N_h-1)d_s\cos\theta}\,]^T, \tag{14}$$

where d_s is the interelement spacing, k is the wave number, and the θ is the angle of the plane wave direction measured from the array axis.

For the interior field, the "traveling" plane waves propagating form each hole to the microphone diaphragm correspond to the array weights vector[22]

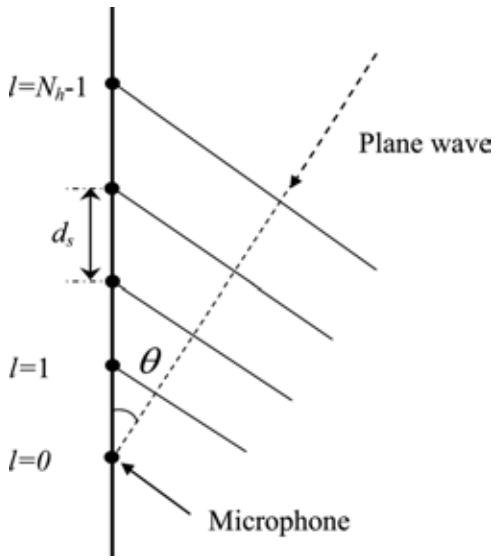

FIG. 2. Modeling the exterior field of a shotgun microphone from an array signal processing perspective.

TABLE I. Parameters of a shotgun tube.

Parameters	Symbol	Value
Tube length	L	0.1 m
Spacing between openings	d_s	0.01 m
Number of holes	N_h	10
Tube thickness	t	0.001 m
Radius of the tube cross-section	r_s	0.0035 m
Radius of the slot openings	r_h	0.000 75 m
Radius of the front-end opening	r_{hf}	0.0035 m

$$\mathbf{w} = [\,1 \quad e^{jkd_s} \quad \cdots \quad e^{j(N_h-1)kd_s}\,]^T. \tag{15}$$

This gives the directional response function of the array

$$H_a(\omega,\,\theta) = \frac{1}{N_h}\mathbf{w}^H\mathbf{a} = \frac{1}{N_h}\sum_{l=0}^{N_h-1} e^{-jkld_s(1-\cos\theta)}, \tag{16}$$

with ω being the angular frequency. Next, we run a simulation using the TWM to calculate the directional response of a shotgun with the tube parameters listed in Table I and omni-microphone parameters listed in Table II. Figure 3 shows the directivity pattern of the shotgun from 500 to 16 000 Hz. The microphone becomes increasingly directional with frequency.

Next a tube mockup with parameters of Table I is constructed and fitted to an omni microphone with parameters of Table II. The experiment is conducted in an anechoic room ($4 \times 5.4 \times 1.9\,\mathrm{m}^3$). The shotgun microphone under test is mounted on an automated turntable. A co-axial full-range loudspeaker (Tannoy V8) is placed at a fixed position. Step-sine signal from 500 to 20 000 Hz in 150 increments is used as the input to measure the frequency response and directivity pattern from 0 to 350° with 10° increments by using a signal analyzer, Pulse (BK 3560C). MATLAB is used for post-processing the acquired data. Figure 4 shows the measured directional response. Marked discrepancy can be observed between the measurement and the prediction by TWM. The model and the experiment are compared quantitatively by the error measure defined as

$$\varepsilon = \frac{\sqrt{\sum_{n=1}^{N}\sum_{m=1}^{M}|p_{sim}(f_n,\theta_m) - p_{mea}(f_n,\theta_m)|^2}}{\sqrt{\sum_{n=1}^{N}\sum_{m=1}^{M}|p_{mea}(f_n,\,\theta_m)|^2}} \times 100\%, \tag{17}$$

TABLE II. Parameters of the base condenser microphone.

Parameters	Symbol	Value
Diaphragm radius	r_D	2 mm
Diaphragm thickness	h_d	2 μm
Built-in stress	σ_T	10 MPa
Air gap distance	h_a	30 μm
Hole radius of backplate	r_h	0.25 mm
Hole number of backplate	N_b	3
Volume of backchamber	V	2×10^{-8} m^3
DC polarization voltage	E	190 V

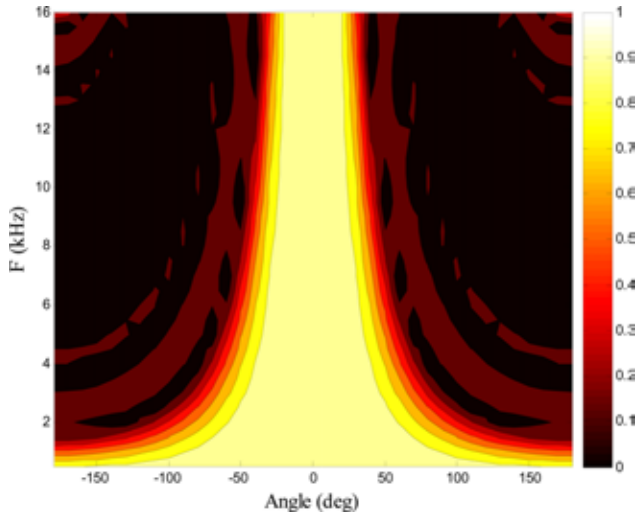

FIG. 3. (Color online) The directional response of a shotgun microphone simulated using the TWM.

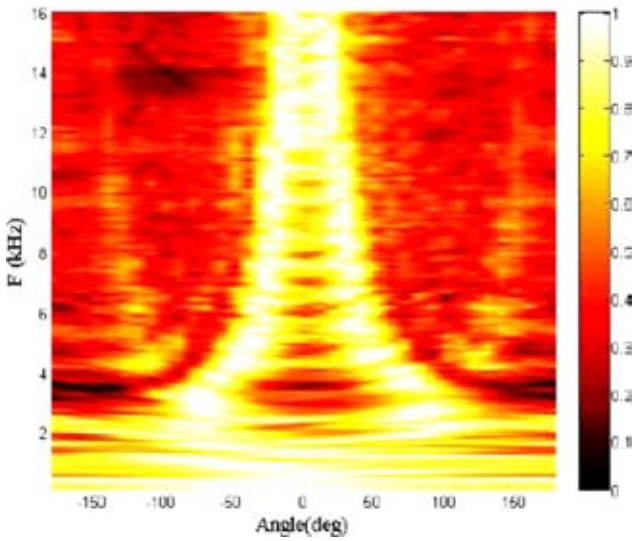

FIG. 4. (Color online) The measured directional response of a shotgun microphone with an omni-directional base element.

where $p_{mea}(f_n, \theta_m)$ and $p_{sim}(f_n, \theta_m)$ are the measured and the simulated microphone outputs at the frequency f_n and angle θ_m. N is the number of frequencies, and M is the number of angles. $\varepsilon = 51.8\%$ between the response predicted by the TWM and the measurement. This comparison suggests that the oversimplified TWM is insufficient to model the shotgun microphone without mesh treatment.

C. Standing-wave model

To better predict the directional response of a shotgun microphone, we propose in the following a refined model, SWM, for the internal field. The SWM is based on the fact that, under the cutoff frequency, the sound field inside a finite-length tube primarily consists of standing waves. To model this, an analogous circuit containing phased pressure sources and T-networks of tube sections is suggested, as shown in Fig. 5. In the analogous circuit, the p_{eq} is the equivalent pressure on the end of the tube in contact with the microphone diaphragm. It represents the voltage drop between the two terminals indicated in the diagram that facilitates the partitioning of the tube circuit and the microphone circuit. For simplicity, we show only the analogous circuit in the acoustical domain, where the incident plane waves are represented by an array of phased pressure sources with unity amplitude

$$p_l = e^{jlkd_s \cos\theta}, \quad l = 0, 1, \ldots, N_h - 1. \tag{18}$$

In addition, T-networks are used to model standing waves in tube segments, where the impedance elements Z_{A1}, Z_{A2}, and Z_{AH} are given by

$$Z_{A1} = j \tan\left(\frac{kd_s}{2}\right) \frac{\rho_0 c}{A_s}, \tag{19}$$

$$Z_{A2} = \frac{-j}{\sin(kd_s)} \frac{\rho_0 c}{A_s}, \tag{20}$$

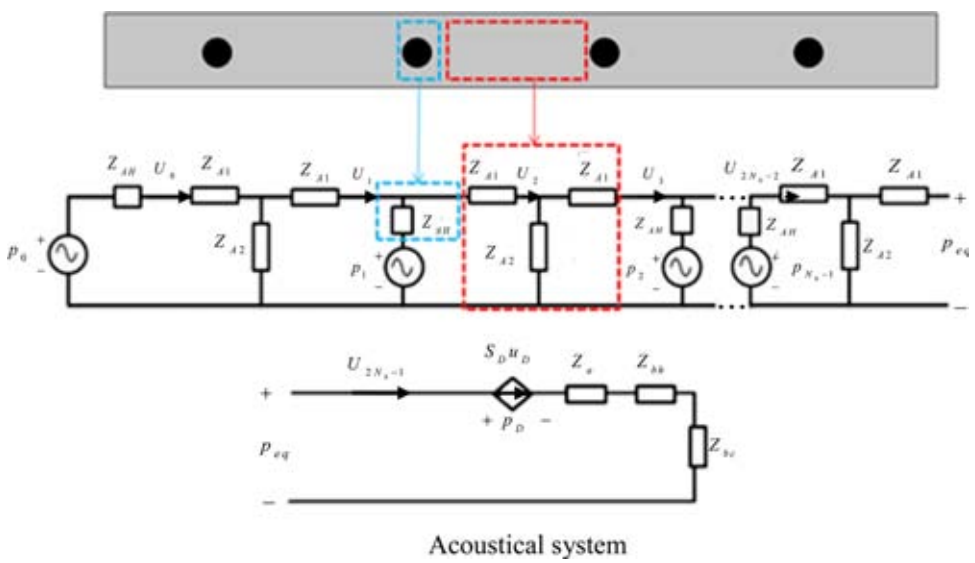

FIG. 5. (Color online) The SWM analogous circuits of the shotgun microphone, including acoustical, electrical, and mechanical domains.

$$Z_{AH} = \frac{\rho_0 c k^2}{2\pi} + j\frac{\omega\rho_0}{\pi a^2}\left(\frac{8a}{3\pi} + t\right), \tag{21}$$

where c is the sound speed, ρ_0 is the air density, A_s is the cross sectional area of a shotgun tube, a is the hole radius on a shotgun, and t is the thickness of a shotgun tube. The incident sound pressures ($\mathbf{p}$) and the unknown volume velocities ($\mathbf{U}$) can be related by the following matrix equation:

$$\mathbf{p}(\omega, \theta) = \mathbf{Z}(\omega)\mathbf{U}(\omega, \theta), \tag{22}$$

where

$$\mathbf{Z}(\omega) = \begin{bmatrix} Z_{sum} & -Z_{A2} & 0 & 0 & 0 & 0 & 0 & 0 \\ Z_{A2} & -Z_{sum} & Z_{AH} & 0 & 0 & 0 & 0 & 0 \\ 0 & -Z_{AH} & Z_{sum} & -Z_{A2} & 0 & 0 & 0 & 0 \\ 0 & 0 & Z_{A2} & -Z_{sum} & Z_{AH} & 0 & \vdots & 0 \\ \vdots & 0 & 0 & \ddots & \ddots & \ddots & \vdots & \vdots \\ \vdots & \vdots & 0 & \vdots & \ddots & \ddots & \ddots & \vdots \\ \vdots & \vdots & \vdots & \vdots & \vdots & -Z_{AH} & Z_{sum} & -Z_{A2} \\ 0 & 0 & 0 & 0 & 0 & 0 & -Z_{A2} & Z_{AM} \end{bmatrix}_{2N_h \times 2N_h}, \tag{23}$$

$$\mathbf{U}(\omega, \theta) = [\,U_0 \quad U_1 \quad \cdots \quad U_{2N_h-1}\,]^T \in \mathbb{C}^{2N_h}, \tag{24}$$

$$\mathbf{p}(\omega, \theta) = [p_0 \quad p_1 \quad p_1 \quad \cdots \quad p_{N_h-1} \quad p_{N_h-1} \quad P_D]^T \in \mathbb{C}^{2N_h}, \tag{25}$$

where $Z_{sum} = (Z_{AH} + Z_{A1} + Z_{A2})$ and $p_D = (-U_{2N_h-1} Z_M / S_D^2)$ with Z_M defined in Eq. (13).

The solution of volume velocities can be obtained by inverting the impedance matrix[28]

$$\mathbf{U}(\omega, \theta) = \mathbf{Z}^{-1}(\omega)\mathbf{p}(\omega, \theta). \tag{26}$$

The average diaphragm velocity can be obtained from the last element of the vector $\mathbf{U}(\omega, \theta)$

$$u_D = \frac{U_{2N_h-1}}{S_D}. \tag{27}$$

Next the open-circuit voltage of the shotgun microphone can be written in terms of the diaphragm velocity above

$$e_{os}(\omega, \theta) = \frac{E}{j\omega h_a} u_D. \tag{28}$$

It follows that the directional response function can be calculated by

$$H_s(\omega, \theta) = \frac{e_{os}(\omega, \theta)}{p_0} = \frac{E u_D}{j\omega h_a p_0}, \tag{29}$$

provided the diaphragm velocity u_D has been obtained from Eq. (27).

The on-axis frequency response of the shotgun microphone is simulated in light of the SWM in Eq. (29). The result shown in Fig. 6 is in reasonable agreement with the measurement. Many resonant peaks are apparently due to the standing waves in the tube. In addition, the directional response simulated in Fig. 7 using the SWM shows the directional response simulated by using the SWM. Here a peculiar phenomenon should be noted in this directional response. There is a discontinuity in the beam pattern at a particular frequency 3278 Hz. In the following presentation, we shall term this phenomenon as *beam pattern bifurcation,* which typically arises at the Helmholtz frequency[16] of the shotgun tube defined as

$$\omega_c = \sqrt{\frac{1}{M_{ht} C_t}}, \tag{30}$$

where $C_t = V_t/(\rho_0 c^2)$ is the effective acoustical compliance due to the tube volume V_t, and M_{ht} is the overall acoustical mass resulting from the slot openings that can be expressed as

$$M_{ht} = \frac{M_{fh} M_h}{M_{fh} + M_h}, \tag{31}$$

where M_{fh} is the radiation mass of the opening at the front end of the tube, and M_h is the radiation mass of the lateral openings defined as follows:

$$M_{fh} = \frac{\rho_0 (t_f + 1.5 a_f)}{\pi a_f^2} \tag{32}$$

and

$$M_h = j\omega \frac{\rho_0 (t + 1.5a)}{(N_h - 1)\pi a^2}, \tag{33}$$

where a_f is the hole radius of the front end of the tube and t_f is the tube thickness. While the shotgun behaves like an end-fire array (with main axis at $\theta = 0°$, 180°) as in the TWM above the Helmholtz frequency, it becomes a broadside array

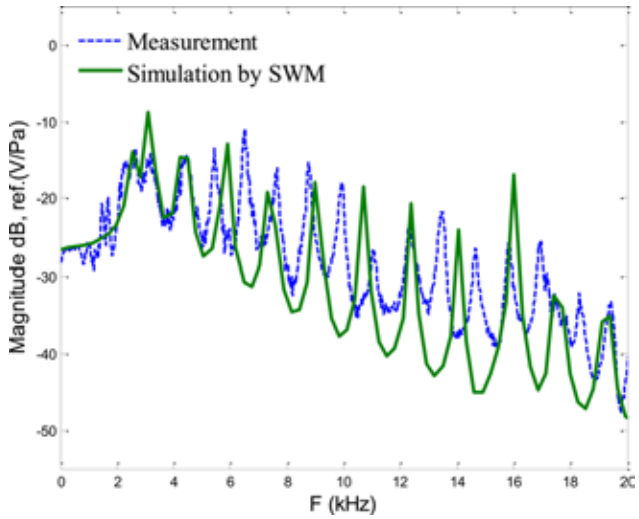

FIG. 6. (Color online) The on-axis frequency response of the shotgun microphone without mesh.

(with main axis at $\theta = \pm 90°$) below the Helmholtz frequency. The standing wave field inside the tube seems to "freeze" the propagation of plane waves. This is one unique characteristic that cannot be predicted by the previous TWM.

Nevertheless, one more refinement is required for the SWM. In the simulated pattern, there seems to be a mirror image between the front and the back of the microphone. This phenomenon, which does not arise in the measurement of Fig. 4, is due to the diffraction effect of the microphone housing, as will be examined next.

III. MODELING DIFFRACTION EFFECTS OF THE HOUSING

The microphone housing is a finite sized object that gives a diffraction pattern with large magnitude in the front and small magnitude in the rear. To model this diffraction effect, the ESM method[12] is used for simulating the directional response, as detailed next.

The idea of ESM is to represent in an equivalent and fictitious sense a sound field by using an array of discrete simple

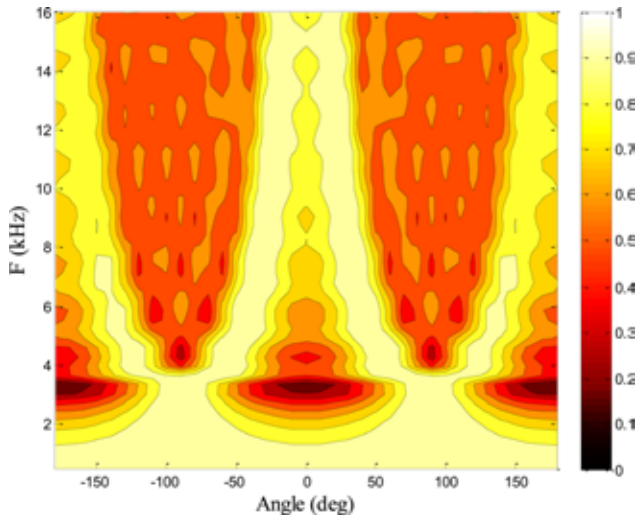

FIG. 7. (Color online) The directional response of the shotgun microphone simulated by the SWM.

sources such as monopoles. Instead of the sensor diffraction problem, we here consider the reciprocal source radiation problem. Except for the front end of the shotgun microphone that is vibrating with a uniform velocity ($u = 1$ m/s), the housing surface is assumed to be rigid elsewhere ($u = 0$ m/s). Suppose that N monopoles with unknown amplitudes are distributed inside the housing surface with appropriate distance. A match condition is imposed that the particle velocities produced by the virtual monopoles have to coincide with given surface velocity distribution at M discrete match points selected in advance. In matrix notation, this can be formulated as[23–25]

$$\mathbf{u}_{na} = \mathbf{G}_{av}\mathbf{a}_s, \tag{34}$$

where $\mathbf{u}_{ns}$ denotes the particle velocity vector at the match points and $\mathbf{G}_{av}$ is a transfer matrix that relates the nth monopole amplitude and the velocity at the mth match point, with the mnth entry defined by

$$\{\mathbf{G}_{av}\}_{mn} = \cos\theta_{mn}\left(\frac{1}{r_{mn}} + jk\right)\frac{e^{-jkr_{mn}}}{j\rho_0\omega r_{mn}}, \tag{35}$$

where r_{mn} is the distance between the nth monopole and the mth match point and θ_{mn} is the subtending angle of the surface normal and the vector connecting the nth monopole and the mth match point. Thus the unknown sourced amplitudes $\mathbf{a}_s$ can be obtained:

$$\mathbf{a}_s = \mathbf{G}_{av}^{+}\mathbf{u}_{ns}, \tag{36}$$

where $\mathbf{G}_{av}^{+}$ signifies the pseudo-inverse of the matrix $\mathbf{G}_{av}$. With these source amplitudes, the pressure field at any points distributed on a farfield circle on the microphone plane and centered at the microphone can be calculated (Fig. 8). The pressure vector of the filed points can be expressed as[26,27]

$$\mathbf{p}_f = \mathbf{G}_{fp}\mathbf{a}_s, \tag{37}$$

where $\mathbf{G}_{fp}$ denotes the transfer matrix from the nth monopole amplitude to pressure of the mth field point with the mnth entry defined by

$$\{\mathbf{G}_{fp}\}_{mn} = \frac{e^{-jkr_{mn}}}{r_{mn}}, \tag{38}$$

where r_{mn} is the distance between the nth monopole and the mth field point on the circle. Therefore the vector $\mathbf{p}_f$ yields a frequency and angle diffraction-dependent pattern $p_f(\omega,\theta)$, which can be multiplied with the SWM pattern to yield the total pressure pattern

$$p_t(\omega, \theta) = p_f(\omega, \theta)H(\omega, \theta). \tag{39}$$

Figure 9(a) illustrates the diffraction pattern $p_f(\omega,\theta)$ calculated by the ESM. Parameters of the ESM are listed in Table III. The retreat distance[17] is chosen to be one lattice spacing between two match points (1 mm). As a refined model with diffraction effect taken into account, the SWM-ESM is

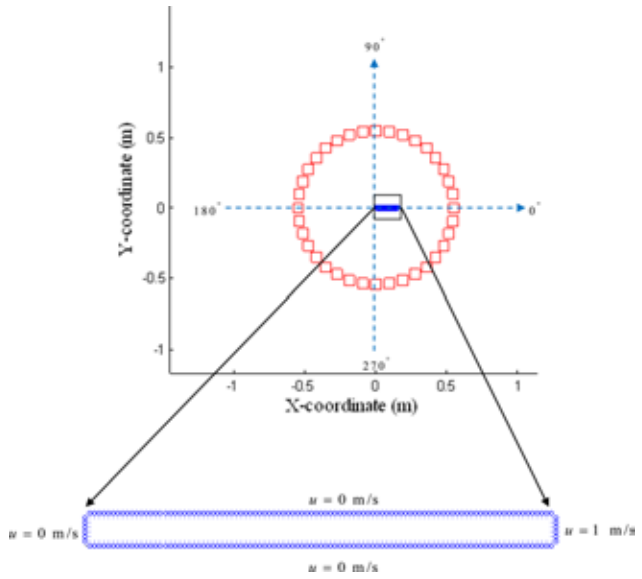

FIG. 8. (Color online) Schematic diagram for modeling diffraction effect using the ESM. (□, field points; ○, match points; ●, equivalent sources)

developed to predict the directional response of the shotgun without mesh as shown in Fig. 9(b). $\varepsilon = 24.7\%$ between the response predicted by the SWM-ESM and the previous measurement in Fig. 4. The SWM-ESM proves to be more accurate than the TWM (24.7% vs 51.8%).

IV. MESH-TREATED SHOTGUN MICROPHONE

It is a common practice that the slot openings are covered with mesh or screen materials to prevent from dust and wind disturbances. It is found from this study that mesh treatment has a profound impact on shotgun microphones.

A. Effects of mesh

We first examine the directional response measurement of a mesh-treated shotgun microphone shown in Fig. 10(a). $\varepsilon = 42.7\%$ between the response predicted by the TWM in Fig. 3 and the measurement in Fig. 10(a). The error between the response predicted by the TWM and the measurement of a mesh-treated shotgun is smaller than that of a shotgun without mesh (42.7% vs 51.8%). This is because standing waves are attenuated by the mesh. The mesh treatment seemed to have mitigated the beampattern bifurcation for some reason. A simulation based on the previous SWM-ESM is carried out to explain this interesting phenomenon. In the simulation, the effective hole radius is reduced to a smaller value 0.1 mm to account for the mesh effect. The directional response simulated is shown in Fig. 10(b). $\varepsilon = 39.4\%$ between the response predicted by the SWM-ESM and the measurement in Fig. 10(a). The SWM-ESM proves to be more accurate than the TWM (39.4% vs 42.7%). As indicated by the directivity index (DI) of Fig. 10(c), the directionality is also considerably enhanced by applying the mesh. The mesh-treated shotgun not only increased the directivity but also revealed a resemblance to the pattern predicted by the TWM in Fig. 3. Nevertheless, the SWM-ESM can still be used to predict

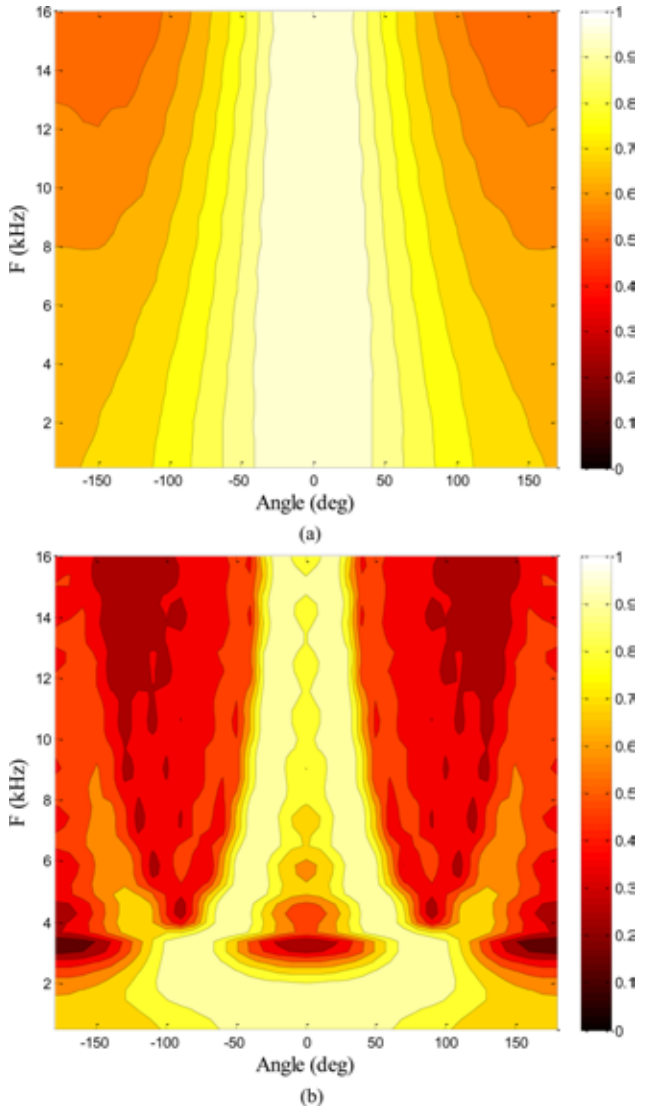

FIG. 9. (Color online) The directional response of the shotgun microphone with diffraction effect taken into account. (a) Diffraction pattern of the shotgun housing calculated by the ESM. (b) The combined directional response of the shotgun microphone simulated using the SWM and ESM.

directional response of the mesh-treated shotgun. Figure 11(a) also shows the on-axis frequency response of the shotgun with mesh treatment. The fundamental frequency is 496 Hz, which is approximately equal to the Helmholtz frequency 459 Hz. With mesh treatment, the Helmholtz frequency is decreased substantially because the effective hole radius, and hence the equivalent acoustical mass, is reduced by the mesh. The on-axis response of the TWM is the product of Eq. (16) and the frequency response of the microphone:

TABLE III. Parameters of ESM.

Parameters	Symbol	Value
Retreat distance	r_t	1 mm
Number of match points	M	210
Number of equivalent sources	N	206

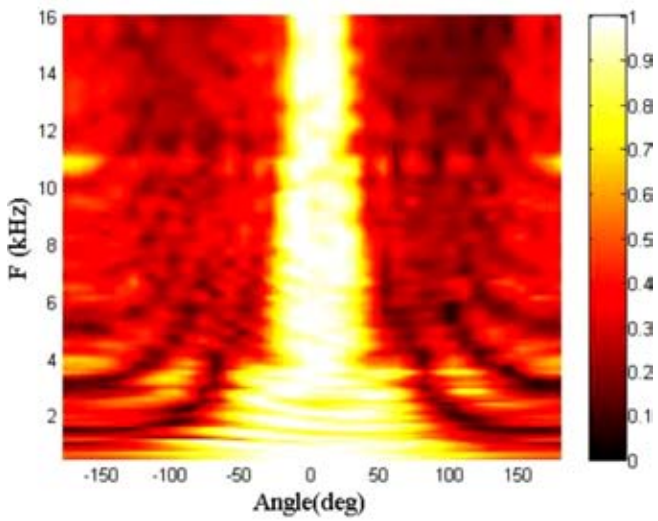

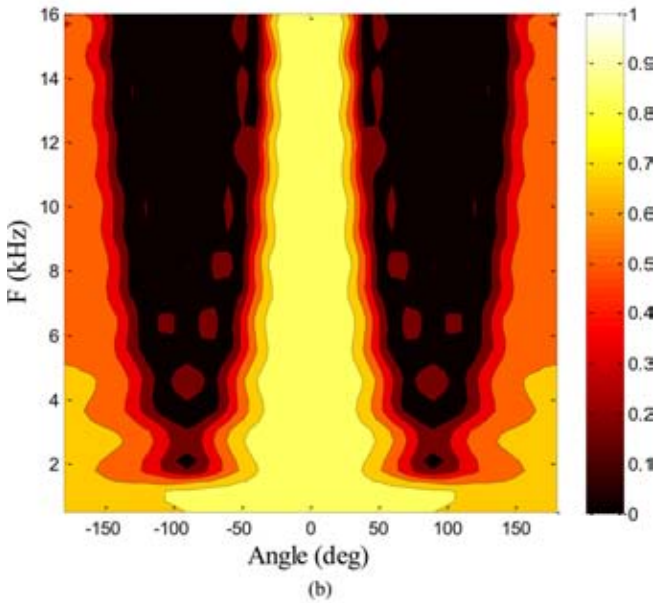

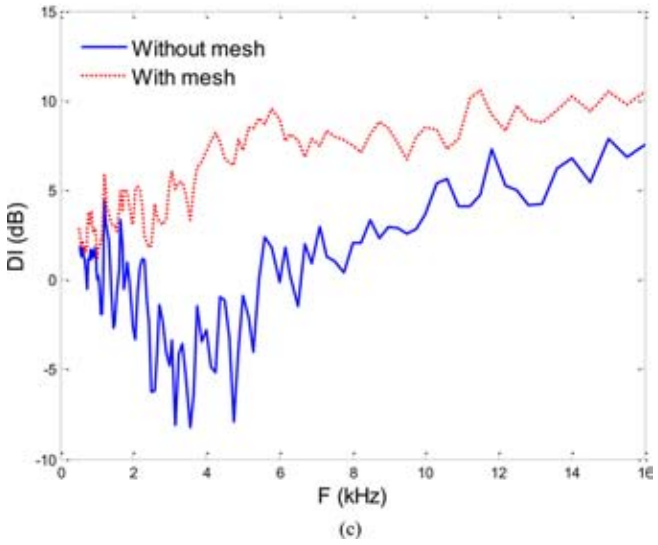

FIG. 10. (Color online) The directional responses of a mesh-treated shotgun. (a) Measurement (b) Simulation based on the SWM and ESM (c) The directivity indices of the shotgun without and with mesh.

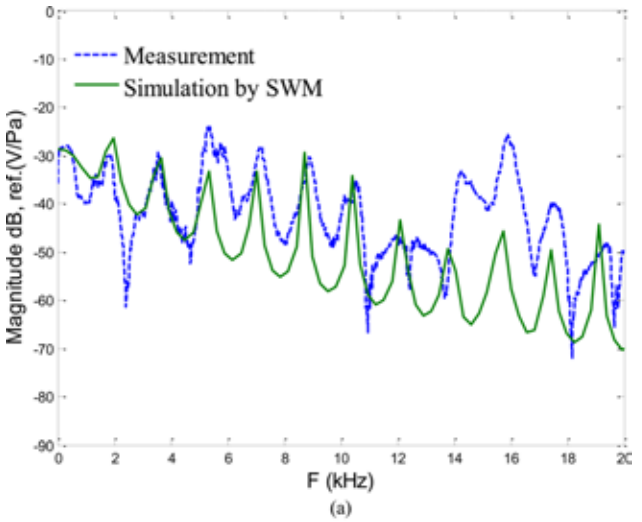

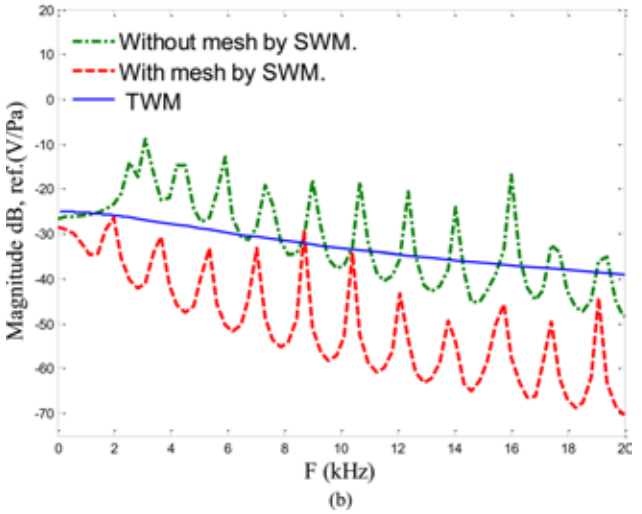

FIG. 11. (Color online) The on-axis frequency response functions of the shotgun. (a) The measurement and simulation based on SWM for the mesh-treated shotgun. (b) The on-axis frequency response functions of shotguns simulated by using SWM and TWM.

$$H_{TWM}(\omega, 0) = H_a(\omega, 0)\frac{e_{om}(\omega)}{p_i(\omega)}. \tag{40}$$

The on-axis responses obtained using TWM and SWM are compared in Fig. 11(b). Resonant peaks are not present in the result of TWM due to its traveling-wave assumption. The simulation results obtained using TWM are the same regardless of mesh treatment. More importantly, the directional pattern approaches that of an endfire array as predicted by the preceding TWM—omni-directional in low frequencies and uni-directional in high frequencies. This observation prompts the development of a mode-switching model, as detailed next.

B. Mode-switching model

The preceding observations can be generalized to a rule of thumb reported in the monograph by Eargle.[1] The directivity of the shotgun below the critical frequency ω_0 (at which the tube length equals half of the wavelength, i.e., $l = \lambda/2$) is that of the base transducer, e.g., a cardioid element. Above the critical frequency, the directional response predicted by

TABLE IV. Parameters of a commercial shotgun tube.

Parameters	Symbol	Value
Tube length	L	0.054 m
Spacing between openings	d_s	0.00215 m
Number of holes	N_h	16

the TWM will become apparent. For mesh-treated shotguns, we propose the following mode-switching model (MSM):

$$H_T(\omega,\,\theta) = H_1(\omega)H_{\mathrm{XDCR}}(\omega,\,\theta) + [1 - H_1(\omega)]\,H_a(\omega,\,\theta), \tag{41}$$

where $H_{\mathrm{XDCR}}(\omega,\theta)$ is the directional response of the base transducer, $H_a(\omega,\theta)$ is the directional response of the shotgun microphone calculated using the foregoing TWM, and $H_1(\omega)$ is a weighting function to "smooth out" the transitional region near the critical frequency ω_0. In this work, the first-order Butterworth window is utilized for $H_1(\omega)$

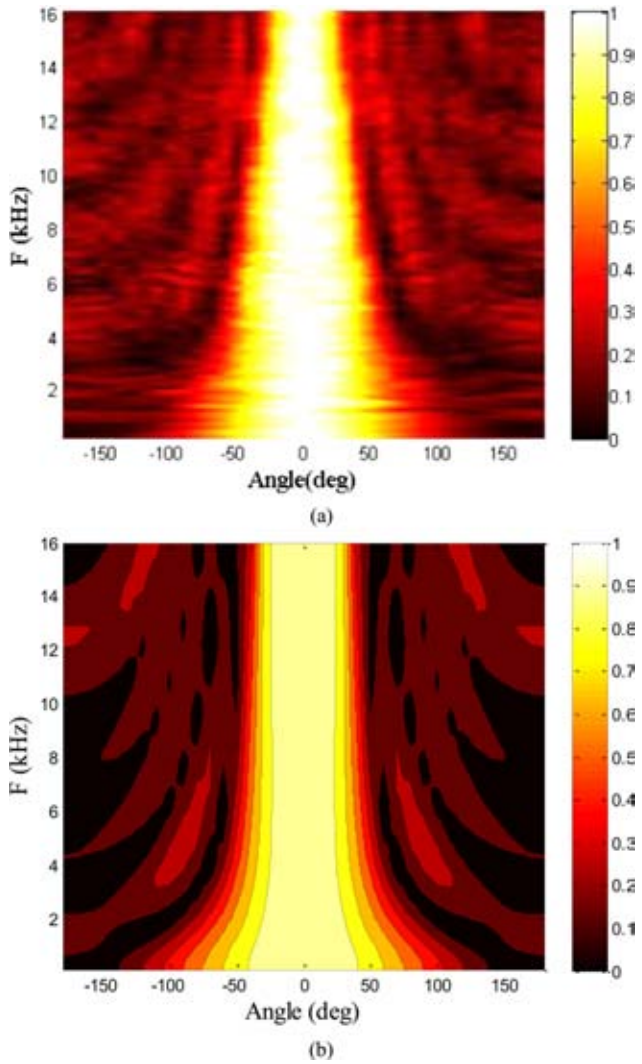

FIG. 12. (Color online) The directional responses of a commercial shotgun microphone (AT9913 of Audio-Technica). (a) Measurement, (b) Simulation based on the MSM.

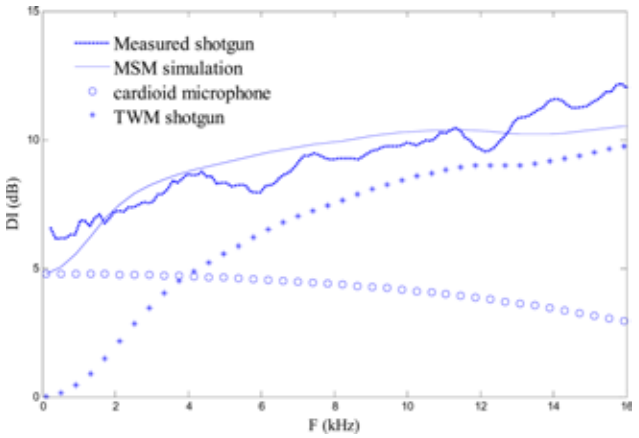

FIG. 13. (Color online) The directivity indexes plotted versus frequency of the shotgun microphone.

$$H_1(\omega) = \sqrt{\frac{1}{1 + (\omega/\omega_0)^2}}. \tag{42}$$

To validate the preceding model, an experiment is conducted for a commercial shotgun microphone (AT9913 of Audio-Technica) that contains a cardioid base element with a slot opening at the back chamber. The effective delay due to the 5.5 mm distance between the microphone diaphragm and the slot leads to the cardioid pattern. The parameters of commercial shotgun microphone are listed in Table IV. Figure 12(a) shows the measured directional response of the microphone. The simulated directional response obtained using the mode-switching model in Eq. (42) with the critical frequency 3118 Hz is shown in Fig. 12(b) for comparison. $\varepsilon = 21.9\%$ between the response predicted by the MSM and the measurement in Fig. 12(a). The MSM has the smallest prediction error (21.9%) among all test cases. The MSM proved effective in predicting the directional response of the commercial shotgun microphone.

The proposed MSM and the measured shotgun microphone response were further compared in terms of DI in Fig. 13, with the DIs of base cardioid microphone and that predicted by the TWM as reference. The difference between DI curves of the MSM prediction and the measurement are within 3 dB throughout the frequency range.

V. CONCLUDING REMARKS

This paper has revisited the analysis and modeling of shotgun microphones. The directional response is influenced by the standing waves, tube resonance, diffraction and phase shift due to propagating delay. Several refinements have been suggested in stages to model the on-axis frequency response and the directional response. The oversimplified TWM proved insufficient for reliable prediction of directional response of a shotgun. To address this issue, the SWM with diffraction effect modeled using ESM have been developed for better prediction of a practical shotgun. The SWM is realized by in light of an analogous circuit containing phased pressure sources and T-networks of tube segments.

The results have revealed that beam pattern bifurcation arises at the Helmholtz frequency. Below this frequency, the responses veer drastically from what is predicted by the TWM. In addition, the study has found that mesh treatment has crucial impact on shotgun microphones. Mesh treatment tends to mitigate the impact of the tube resonance and beam pattern bifurcation and to enhance the directivity of the shotgun microphone. At high frequencies, the shotgun tends to the performance predicted by the TWM. At low frequencies, however, the directional response of the shotgun reduces to that of the base transducer. The MSM has been suggested to predict the directional responses of mesh-treated shotguns with satisfactory accuracy.

ACKNOWLEDGMENT

The work was supported by the National Science Council in Taiwan, Republic of China, under the Project No. NSC94-2212-E-009-018.

[1]J. Eargle, *The Microphone Book* (Focal Press, Waltham, MA, 2005), pp. 108–114.
[2]H. F. Olson, "Line microphones," Proc. IRE **27**, 438–446 (1939).
[3]H. F. Olson, "Directional microphones," J. Audio Eng. Soc. **15**, 420–430 (1967).
[4]H. F. Olson, "The quest for directional microphones at RCA," J. Audio Eng. Soc. **28**, 776–786 (1980).
[5]W. P. Mason and R. N. Marshall, "A tubular directional microphone," J. Acoust. Soc. Am. **10**, 206–215 (1939).
[6]T. N. Carnes, D. D. Reynolds, and E. L. Hixson, "Analytical modeling of wave interference directional microphones," J. Eng. Ind. **103**, 361–371 (1981).
[7]G. Ballou, J. Ciaudelli, and V. Schmitt, *Electroacoustic Devices: Microphones and Loudspeakers* (Focal Press, Waltham, MA, 2009), pp. 82–89.
[8]G. R. Dix, "Development and comparison of highly directional loudspeakers," M.S. thesis, Brigham Young University, Provo, UT, 2006.
[9]W. M. Leach, Jr., *Introduction to Electroacoustics and Audio Amplifier Design*, 3rd ed., (Kendall/Hunt Publishing, Dubuque, IA, 2003), pp. 33–83.
[10]G. S. K. Wong and T. F. W. Embleton, *AIP Handbook of Condenser Microphones* (AIP, Melville, NY, 1994), pp. 37–68.
[11]C. W. Tan and J. Miao, "Analytical modeling for bulk-micromachined condenser microphones," J. Acoust. Soc. Am. **120**, 750–761 (2006).
[12]Y. B. Zhang, F. Jacobsen, C. X. Bi, and X. Z. Chen, "Near field acoustic holography based on the equivalent source method and pressure-velocity transducers," J. Acoust. Soc. Am. **126**, 1257–1263 (2009).
[13]W. J. Wang, R. M. Lin, Q. B. Zou, and X. X. Li, "Modeling and characterization of a silicon condenser microphone," J. Micromech. Microeng. **14**, 403–409 (2004).
[14]M. Pedersen, "A polymer condenser microphone realized on silicon containing preprocessed integrated circuits," Ph.D. thesis, University of Twente, Enschede, Netherlands, 1997.
[15]M. Pedersen, W. Olthuis, and P. Bergveld, "A silicon condenser microphone with polyimide diaphragm and backplate," Sens. Actuators, A **63**, 97–104 (1997).
[16]R. L. Panton and J. M. Miller, "Resonant frequencies of cylindrical Helmholtz resonators," J. Acoust. Soc. Am. **57**(6), 1533–1535 (1975).
[17]M. R. Bai, C. C. Chen, and J. H. Lin, "On optimal retreat distance for the equivalent source method-based nearfield acoustical holography," J. Acoust. Soc. Am. **129**(3), 1407–1416 (2011).
[18]M. Bao, H. Yang, Y. Sun, and Y. Wang, "Squeeze-film air damping of thick hole-plate," Sens. Actuators, A **108**, 212–217 (2003).
[19]D. Homentcovschi and R. N. Miles, "Modeling of viscous damping of perforated planar microstructures. Applications in acoustics," J. Acoust. Soc. Am. **116**, 2939–2947 (2004).
[20]D. Homentcovschi and R. N. Miles, "Analytical model for viscous damping and the spring force for perforated planar microstructures acting at both audible and ultrasonic frequencies," J. Acoust. Soc. Am. **124**, 175–181 (2008).
[21]C. W. Tan and J. Miao, "Modified Škvor/Starr approach in the mechanical-thermal noise analysis of condenser microphone," J. Acoust. Soc. Am. **126**, 2301–2305 (2009).
[22]H. F. Olson, "Gradient loudspeakers," J. Audio Eng. Soc. **21**, 86–93 (1973).
[23]E. G. Williams, *Fourier Acoustics: Sound Radiation and Nearfield Acoustica Holography* (Academic, San Diego, 1999), pp. 149–291.
[24]N. P. Valdivia and E. G. Williams, "Study of the comparison of the methods of equivalent sources and boundary element methods for near-field acoustic holography," J. Acoust. Soc. Am. **120**, 3694–3705 (2006).
[25]J. Gomes, J. Hald, P. Juhl, and F. Jacobsen, "On the applicability of the spherical wave expansion with a single origin for near-field acoustical holography," J. Acoust. Soc. Am. **125**, 1529–1537 (2009).
[26]F. Jacobsen and Y. Liu, "Near field acoustic holography with particle velocity transducers," J. Acoust. Soc. Am. **118**, 3139–3144 (2005).
[27]S. F. Wu, "Methods for reconstructing acoustic quantities based on acoustic pressure measurements," J. Acoust. Soc. Am. **124**, 2680–2697 (2008).
[28]B. Noble and J. W. Daniel, *Applied Linear Algebra*, 3rd ed. (Prentice-Hall, Englewood Cliffs, NJ, 1988), pp. 271–272.